Journal of
Ceramic Science
and Technology

J. Ceram. Sci. Technol., **13** [1] 15-22 (2022)
DOI: 10.4416/JCST2021-00011
available online at: http://www.ceramic-science.com

Effect of the Addition of Ultrafine Powders on the Microstructure and Mechanical Properties of TiCN-Based Cermets

Y. Yang[1, 2], W. Dang[1, 2], J. Liu[1, 2], H. Zhang[*1, 2], S. Gu[1, 2], C. Lei[1, 2], Y. Chen[1, 2]

[1]Fujian Key Laboratory of Functional Materials and Applications, Xiamen University of Technology, Xiamen 361024, Fujian, P.R. China
[2]Xiamen Key Laboratory for Power Metallurgy Technology and Advanced Materials, Xiamen University of Technology, Xiamen 361024, Fujian, P.R. China
received July 18, 2021; received in revised form November 2, 2021; accepted November 7, 2021

Abstract

In this study, ultrafine titanium carbonitride (TiCN) powders were prepared with an improved carbothermal reduction method. The microstructure and mechanical properties of TiCN-based cermets fabricated with different contents of ultrafine powders were investigated by means of scanning electron microscopy, X-ray diffraction, Vickers hardness and three-point bending tests. With the addition of ultrafine TiCN powder, the "black core-grey rim" phase was refined, and the "white core-grey rim" phase was gradually produced. The optimum content of ultrafine TiCN powder is 20 wt%. The cermets' hardness, bending strength and fracture toughness were increased by 2.5 %, 7.9 % and 20.4 %, respectively, compared to those without the addition of the ultrafine TiCN powders. The enhanced mechanical properties were attributed to fine grain strengthening, microcrack toughening, crack deflection and crack microbridging. In summary, a reasonable mixture of ultrafine TiCN and micron TiCN powders was beneficial to improve the comprehensive properties of TiCN-based cermets.

Keywords: Ultrafine TiCN powders, cermets, microstructure, mechanical properties

I. Introduction

TiCN-based cermets have been widely used in finishing and semi-finishing owing to their excellent mechanical properties and oxidation resistance. Two phases have been observed and reported to be contained in TiCN-based cermets. One is the hard ceramic phase composed of TiCN and its solid solution, and the other is the ductile metal binder phase such as Ni and Co [1]. The synergistic effect of these two phases endows TiCN-based cermets with excellent red hardness, good wear and oxidation resistance, and superior chemical stability [1,2]. The abrasion resistance of TiCN-based cermets is much higher than that of WC-Co hard metal. Tools made of TiCN cermet endure a higher cutting speed and have a longer service life [2]. Particularly, the lower production cost of TiCN-based cermets makes them a more competitive alternative to WC and other cemented carbide materials [3]. However, compared with traditional WC-Co cemented carbide materials, the strength and toughness of TiCN-based cermets are still insufficient, which greatly limits their application [3].

The fracture toughness of TiCN-based cermets refers to their ability to resist crack propagation, which is mainly determined by the sintering process, chemical composition, secondary carbide additive, and the particle size of the raw material powders [4–6]. In recent years, research on toughening TiCN-based cermets has attracted increasing interest. Xu *et al.* [7] have developed a new method for the preparation of highly toughened TiCN-based cermets. These cermets are composed of a single solid-solution phase fabricated by means of mechanical activation and *in-situ* carbothermal reduction. The fracture toughness of the as-prepared TiCN-based cermets can reach 21.3 MPa $\cdot m^{1/2}$, which is 66.4 % higher than that of traditional cermets. Yang *et al.* [8] have fabricated TiB_2-TiCN-(Ni+Co) cermets by means of reactive hot pressing. They have demonstrated that the strength and toughness of TiB_2-TiCN-Ni cermet with 2 wt% Mo addition could be simultaneously improved based on the refining of the ceramic particles, the achievement of a homogeneous microstructure, and the enhancement of interfacial bonding. Xiong *et al.* [9,10] have conducted a detailed study on the enhanced interface effect of secondary cubic carbides on TiCN-based cermets. They found that VC reduced the lattice mismatch effectively between the core and rim microstructure, and that the bending strength and fracture toughness of the TiCN-based cermets reached 2 099 MPa and 10.3 MPa$\cdot m^{1/2}$, respectively. Moreover, (Ti, W) (C, N)-based cermets possessing good toughness were fabricated with the use of ultrafine or nanocrystalline (Ti, W) (C, N) powders [11,12]. With the addition of nanoparticles to the raw material powders, the nanoparticles in TiCN-based cermets were embedded in the rim of the larger ceramic grains, bonding the large ceramic particles together and enhancing the toughness of the cermet [13]. Unfor-

* Corresponding author: ha_zhang@163.com

tunately, the increasing fractions of interfaces led to the increase of cracks along the grain boundaries when the particle size was reduced to the nanoscale. It has been reported that the toughness of TiCN-based cermets cannot be improved ultimately [14]. Therefore, the key problem to improve the toughness of cermet materials is how to reasonably control the particle size in the raw material. As we have seen, there is a lack of studies on how the particle size controls the mechanical properties of TiCN-based cermets.

Recently, the *in-situ* carbothermal reduction method has been well developed to synthesize TiCN powders using TiO_2 and carbon black as raw materials [15–18]. Owing to the difference in density and polarity between TiO_2 and carbon black, it is difficult to mix them uniformly using the traditional carbothermal reduction method. In this study, the ultrafine TiCN powders were prepared with an improved carbothermal reduction method. The carbon black was added into $TiCl_4$ solution, so that TiO_2 nanoparticles obtained by hydrolysis-precipitation could be evenly and fully mixed with the carbon source. Then the as-prepared TiCN powders were used as raw materials or additives to prepare the TiCN-based cermets. In addition, we investigated how the content of ultrafine TiCN powder affects the microstructure and mechanical properties of the cermets.

II. Experimental Procedure

(1) Synthesis of ultrafine TiCN powders

The ultrafine TiCN powders were prepared with the improved *in-situ* carbothermal reduction method. First, $TiCl_4$ was added into the mixed solution of ethanol and cyclohexane, and the mixture was continuously stirred to prepare solution A. Then the carbon black and hexadecyl trimethyl ammonium bromide were added to a mixture of ethanol and deionized water, respectively, to obtain solution B. The two kinds of solution B and A were evenly mixed, whilst dilute ammonia solution was slowly dropped into the mixed solution. After neutralization had been completed, the suspension was filtered, and the solid powders were washed and dried to obtain the precursor powders. Finally, the precursor powders were put into a vacuum sintering furnace. At 1 000 °C, the roots pump was shut down and nitrogen was injected. The nitrogen pressure was stabilized at 1 500 ~ 2 000 Pa, and the heat preservation temperature was 1 530 °C for 4 h. The ultrafine TiCN powders measuring 200 ~ 300 nm in size were synthesized, and the purity of powders was over 99.3 %.

(2) Preparation of TiCN-based cermets

Two types of TiCN-based cermets have been prepared and investigated in this study:(1) One used ultrafine TiCN powders (200 ~ 300 nm) as raw material; and (2) the other used the mixture of ultrafine TiCN powders (200 ~ 300 nm) and micron TiCN powders (2 ~ 5 μm) as raw materials. In Situation 1, WC (20 ~ 40 μm), Mo_2C (2 ~ 5 μm) and NbC (1 ~ 2 μm) powders were used as the secondary carbides, and Co and Ni powders (0.8 μm) were used as the binder metals. TiCN-20WC-10Mo_2C-5NbC-15(Co+Ni) cermet (named A in Table 1) can be obtained. In Situation 2, the detailed compositions for preparation of the TiCN-based cermets (named B1 – B6) are shown in Table 1. In order to discuss the influence of content and size of the WC powders, fine WC powders (2 ~ 5 μm) were selected as the raw carbide powders in the B1 – B6 cermets and their content was 15 wt%. The preparation process for the TiCN-based cermets can be described based on the following experimental steps: First, according to the designed composition, each component powder was weighed on an analytical balance. Then, the mixture was ball-ground in a planetary ball mill (QM-LSP), with a stainless steel ball grinding tank and WC-Co cemented carbide balls as the abrasive and anhydric ethanol as the ball grinding medium. The ball to material ratio was 7:1 and the ball grinding speed was 200 r/min over a duration of 30 hours. After ball grinding, the slurry was put into the air-blast drying oven and the drying temperature was 70 °C. The dried powder was screened on a 60-mesh screen and granulated with 6 % paraffin as moulding agent. Unidirectional pressing was carried out on a powder tablet press (769YP-30T). The pressing force was about 250 MPa, and the size of the shaped compact was 8.56 mm × 25.5 mm. Finally, the formed billet was sintered in the vacuum furnace at 1 350 °C ~ 1 475 °C for 1 hour.

Table 1: Composition design of the TiCN-based cermets (wt%).

Cermets	WC	Micron TiCN	Ultrafine TiCN	Mo_2C	NbC	Co+Ni
A	20	0	50	10	5	15
B1	15	50	0	10	5	20
B2	15	45	5	10	5	20
B3	15	40	10	10	5	20
B4	15	30	20	10	5	20
B5	15	20	30	10	5	20
B6	15	0	50	10	5	20

(3) Characterization

The phase structure of the TiCN-based cermets was measured using an X-ray diffractometer (XRD, PANalytical, X'Pert PRO, Netherlands) with $CuK_{\alpha 1}$ radiation (λ = 1.54056 Å) at 40 kV and 30 mA over a 2-theta range from 5° to 90°, and the scanning speed was 0.02(°)/s. The microstructure of the polished cermets was examined with a field emission scanning electron microscope (SEM, Zeiss Sigma 500, Germany) equipped with energy-dispersive spectroscopy (EDS, Oxford Instrument X-max N, UK). The fracture morphology and microstructure were observed under a backscattered electron mode. The density of the sample was measured according to Archimedes' law. The hardness (HV_{30}) of TiCN-based cermets was measured on a Vickers hardness tester, with a regular four-pyramid diamond indenter with a load of 294 N for 15 s. A universal electronic testing machine was used to mea-

sure the three-point bending strength of the cermets. The loading speed of the equipment was 1 mm·min^{-1}, and the span of cemented carbide mould was 12 mm. The indentation fracture toughness of cermets was calculated according to the following equation, as specified in previous studies [19–21]:

$$K_{IC} = 0.15\sqrt{\frac{HV_{30}}{\sum_{i=1}^{4} l_i}}$$

where HV_{30} is the Vickers hardness (N/mm^2) and l_i is the length of the crack tip from the hardness indentation (mm).

III. Results and Discussion

(1) Phase structure analysis

Fig. 1(a) shows the XRD patterns of Cermet A sintered at temperatures ranging from 1 350 °C to 1 475 °C for 1 hour. (W, Mo, Ti, Nb)(C, N) phase. Co/Ni solid solution phase was detected in a sample sintered at 1 350 °C for 1 hour. It has been reported that when the proportion of W, Mo and other atoms in cermets is too high, the excess W, Mo and other atoms will not dissolve into (Ti, Me) (C, N) phase again. They dissolve into the Co/Ni binding phase, and form the secondary phase such as (W, Mo, Ti) (Co, Ni)C [22]. In this study, the (W, Mo, Ti, Nb) (Co, Ni)C phase was found when the sample was sintered at 1 350 °C. As the sintering temperature increased, the diffraction peak of (W, Mo, Ti, Nb)(Co, Ni)C phase tended to weaken, and disappeared when the temperature reached 1 475 °C. The ratio of intensity for (111) planes to (200) planes of (Ti, Me)(C,N) phase changed from 0.608 at 1 350 °C to 1.073 at 1 475 °C. In general, the (111) plane in TiCN unit cell is mainly composed of Ti atoms, while the (200) crystal surface is composed of Ti, C and N atoms together [23, 24]. When W, Mo, Ta, Nb and other metal atoms diffuse into the TiCN lattice, foreign metal atoms are more likely to replace Ti atoms in (111) planes than in (200) planes, resulting in an increase in the ratio of the intensity of the (111) peak to the (200) peak [23]. This also shows that more W, Mo, Nb atoms are dissolved into (Ti, Me)(C, N) phase when the sintering temperature rises.

The XRD patterns of cermets B1-B6 with different contents of ultrafine TiCN powders sintered at 1 450 °C for 1 hour are shown in Fig. 1(b). The cermets under each component consist of two phases, one is the (Ti, Me)(C, N) (Me = W, Mo, Nb) phase, and the other is the Co/Ni solid solution phase, indicating that a good solid solution between the carbides can be formed in the cermets after these are sintered at 1 450 °C for 1 hour. With the increase of the content of ultrafine TiCN powders in the raw material, the ratio of the diffraction intensity between (111) and (200) plane in the cermet also increases. This further confirmed that more W, Mo, Nb atoms were dissolved into the (Ti, Me) (C, N) phase as the amount of the ultrafine TiCN powder increased. According to the comparison between Fig. 1(a) and (b), Cermet A still has a certain amount of (W, Mo, Ti, Nb)(Co, Ni)C phase at 1 450 °C, which, however, disappears at 1 475 °C, while Cermet B6 has no (W, Mo, Ti, Nb)(Co, Ni)C phase after sintering at 1 450 °C. This indicates that finer WC powder and lower content of WC are beneficial to promote the solid solution of W atoms, thus avoiding the formation of (W, Mo, Ti, Nb)(Co, Ni)C phase.

(2) Microstructure and chemical composition

Fig. 2 shows the backscattered electron images of the Cermet A obtained at different sintering temperatures for 1 hour. In Fig. 2(a), a large amount of white phase and "black core-grey rim" phase was observed in the microstructure of cermet. With the increase of sintering temperature, the fractions of the white phase decreased gradually in Fig. 2(b) to 2(d). The EDS analysis results of the Cermet A sintered at 1 425 °C for 1 hour are shown in Table 2. It can be seen that the main elements in the white

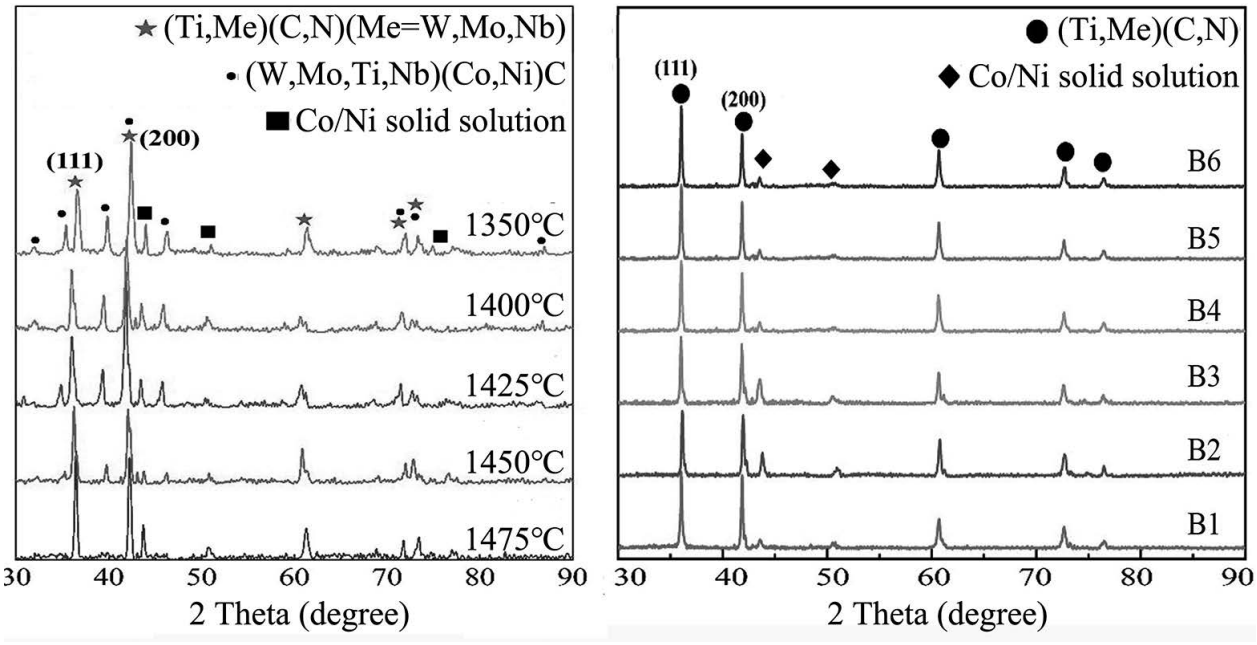

Fig. 1: The XRD patterns of cermet A sintered at different temperatures for 1 h (a) and Cermet B1 – B6 sintered at 1 450 °C for 1 h (b).

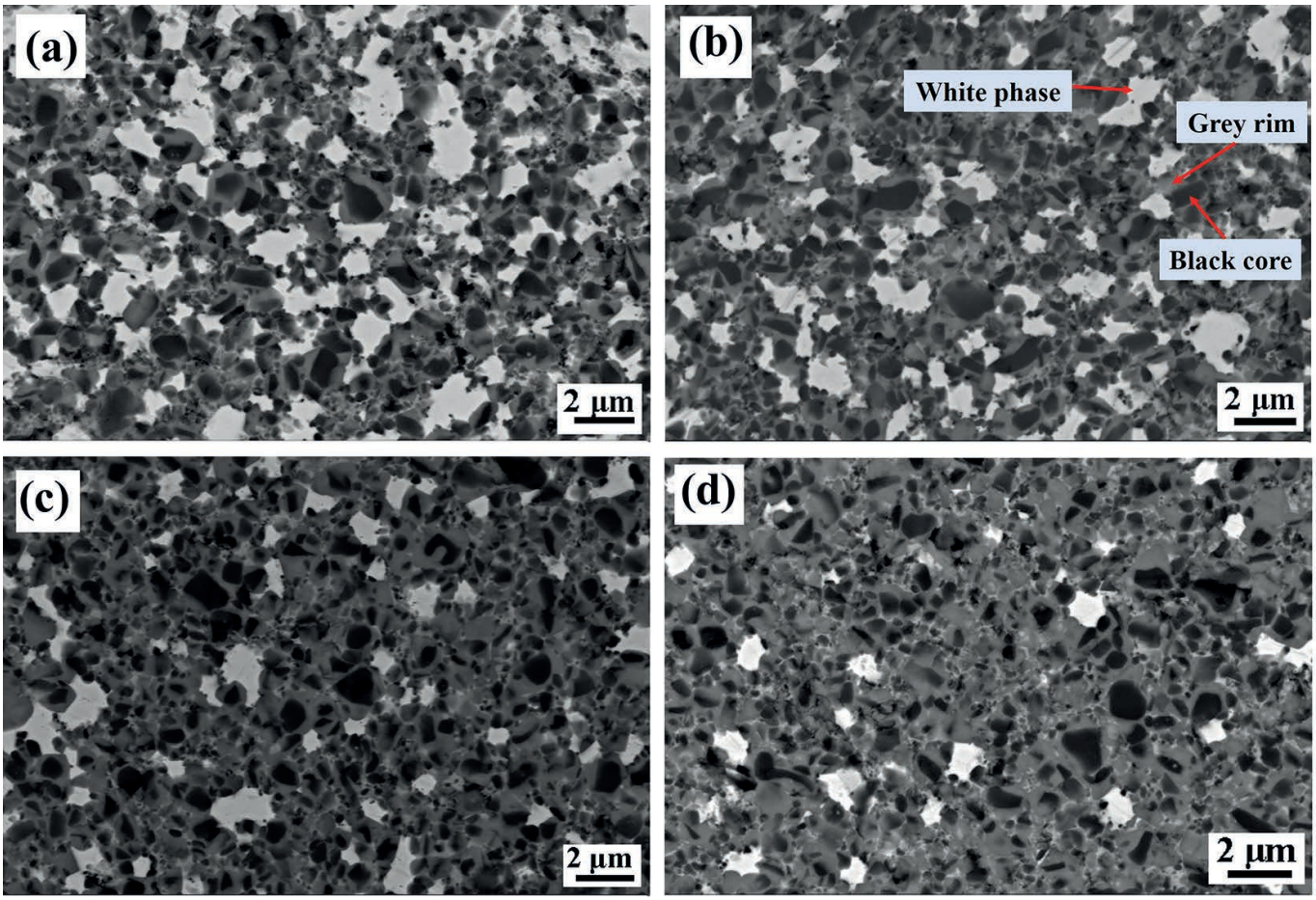

Fig. 2: The backscattered electron SEM images of Cermet A obtained at different sintering temperatures for 1 h. (a) 1 400 °C, (b) 1 425 °C, (c) 1 450 °C, (d) 1 475 °C.

phase are W, Ti, Mo, Co, Ni and a small amount of Nb. The contents of W and Mo are very high. According to Fig. 1(a), the white phase is (W, Mo, Ti, Nb)(Co, Ni)C.

The formation mechanism of "black core-grey rim" in TiCN-based cermets has been reported to follow the principle of "dissolution-reprecipitation" [25,26]. In the solid solution of (W, Mo, Ti, Nb) (C, N), the binding force between Mo-C,W-C and Nb-C is weaker than that between Ti-C, thus W, Mo and Nb can dissolve more easily into the binder phase during the high-temperature liquid-phase sintering. During the cooling process, W, Mo, Ti and Nb become oversaturated in the binder phase owing to the low solubility, and gradually precipitate out of the binder phase and nucleate on the surface of the insoluble (W, Mo, Ti, Nb) (C, N) to form the coated phase. Owing to the difference in solubility, the content of W and Mo in the precipitated phase is higher than that of the black core, so the rim phase appears grey relative to the black core phase. It is believed that the "black core" is an undissolved TiCN particle, and the mass fraction of Ti in the metal elements of the black core phase can be as high as 97 % [27]. However, in this study, the mass fraction of Ti in the black core phase is only 55.95 % (37.17 at% in Table 2). The reason for this phenomenon may be that the ultrafine TiCN powders used in this study are more likely to form a solid solution with the elements W, Mo and Nb.

Fig. 3 shows the backscattered electron images (BSE) of the TiCN-based cermets with different components sintered at 1 450 °C for 1 hour. No coarse-grained (W, Mo, Ti, Nb)(Co, Ni)C phases appear in the microstructure of Cermets B1 – B6. As shown in Fig. 3(a), the larger-sized "black core I-grey rim" phase is formed in Cermet B1 without the addition of ultrafine TiCN powders. When the content of ultrafine TiCN powders is 5 wt%, the amount of larger-sized "black core I-grey rim" phase is reduced, and the smaller-sized "black core II-grey rim" phase appeared. The EDS results are shown in Table 3. The mass fraction of Ti in the phase of black core I accounts for 78.76 % (55.64 at%), while that in black core II accounts for 40.51 % (34.71 at%). This is because the composition of the phase is mainly derived from the micron-sized TiCN powder in black core I. These micron-sized TiCN powders have larger particles that are difficult to dissolve completely, resulting in the main metal element of Ti in the core. The main composition of the phase in black core II is from the ultrafine TiCN powder with larger specific surface area, which more readily forms the solid solution with WC, NbC, Mo_2C and other carbides. As a result, in addition to Ti element, other metal elements such as W, Nb and Mo exist in the black core II. A gradual increase of the fine "white core-grey rim" phase can be observed in Fig. 3(b) – (f). It is mainly caused by the

Table 2: The element content for Cermet A sintered at 1 425 °C for 1 h (at%).

Element (at%)	N	Ni	C	Ti	W	Mo	Nb	Co
White phase	6.51	6.81	46.19	4.73	14.91	9.83	0.59	10.43
Black core	19.82	1.02	36.59	37.17	1.87	1.18	0.83	1.53
Grey rim	21.41	1.36	38.66	31.36	3.04	1.73	0.51	1.93

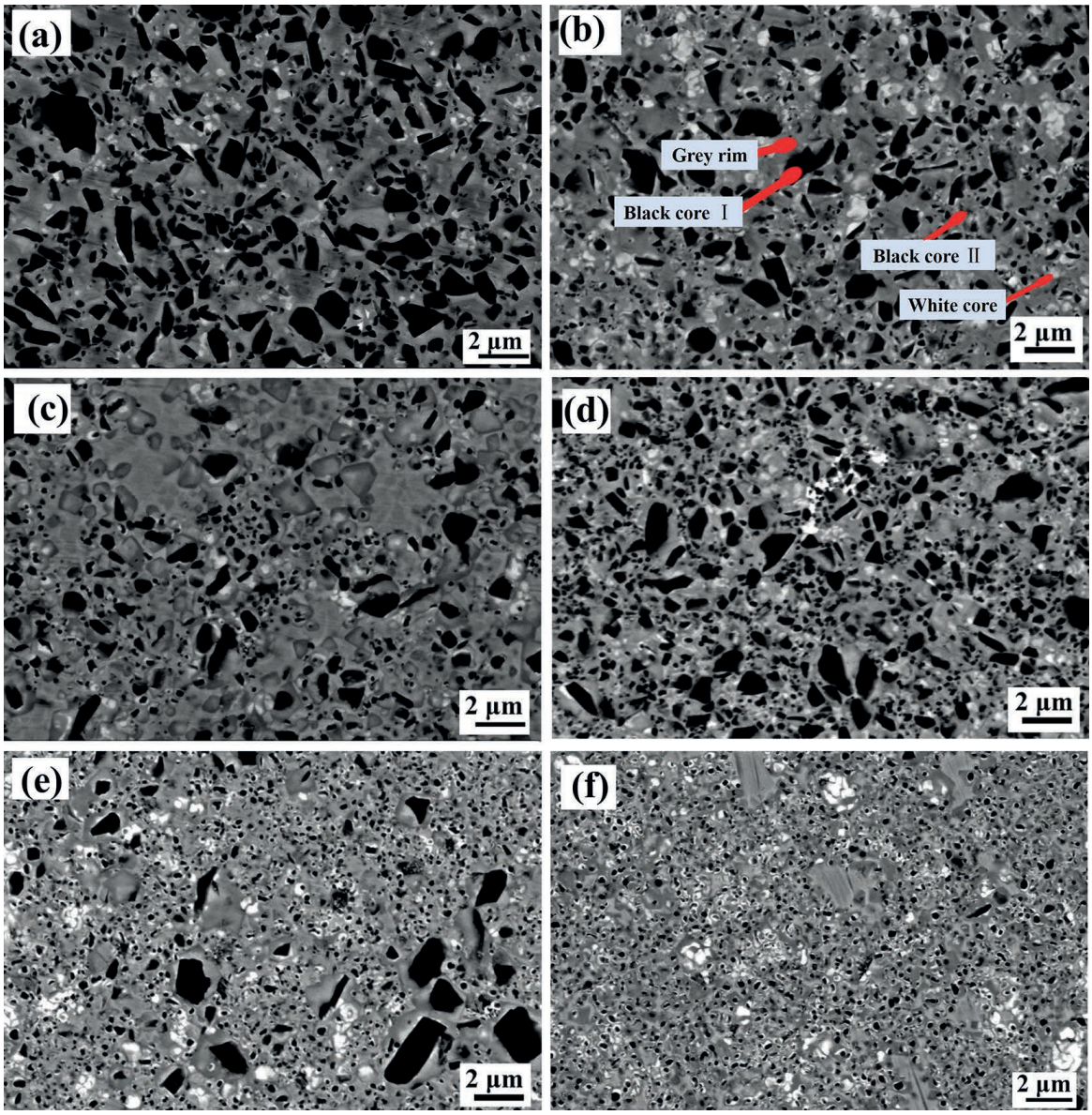

Fig. 3: The backscattered electron SEM images of the TiCN-based cermets with different components sintered at 1 450 °C for 1 h. The content of ultrafine TiCN powders is (a) 0 wt%, (b) 5 wt%, (c) 10 wt%, (d) 20 wt%, (e) 30 wt%, (f) 50 wt%.

Table 3: The element content for Cermet B1 – B6 sintered at 1 450 °C for 1 h.

Element (at%)	N	Ni	C	Ti	W	Mo	Nb	Co
Black core I	10.38	0.13	32.47	55.64	0.56	0.40	0.24	0.17
Black core II	8.67	0.27	42.76	34.71	5.73	5.33	2.19	0.33
Grey rim	3.64	1.42	58.57	25.11	3.54	3.84	1.86	2.02
White core	3.44	6.97	54.07	3.53	10.00	13.41	0.54	8.04

dissolution of ultrafine TiCN, WC, Mo_2C, NbC and other carbides in the binder to form a solid solution phase with high W and Mo content. With the increase in the fractions of ultrafine TiCN powders, the microstructure of TiCN-based cermets has been refined. The amount of larger black core phase decreases gradually, whiles the amount of finer black core and white core increases. When the content of ultrafine TiCN is 50 wt%, the coarse "black core-grey rim" phase can no longer be observed in the microstructure of the cermet. It is composed of finer "black core-grey rim" phase and "white core-grey rim" phase (Fig. 3(f)).

(3) Mechanical properties

The relative density of TiCN-based cermets with different components is shown in Fig. 4(a). The density of the cermet firstly increases and then decreases with the increase of the content of ultrafine TiCN powders. When the content of ultrafine TiCN powders is 20 wt%, the relative density reaches the highest value of 99.6 %. The main reason is attributed to the match between micron-sized particles and ultrafine TiCN particles. It is known that the relative density of TiCN-based cermets is mainly determined by the "dissolution-reprecipitation" mechanism and the rearrangement of hard phase particles during the liquid sintering process [5]. Under the action of surface tension and capillary force in the liquid phase, the carbonitride hard phase particles can undergo a rearrangement process to obtain densification. The ultrafine TiCN powder has a higher dissolution rate, which can promote the "dissolution-reprecipitation" process of the carbonitride hard phase. Moreover, the ultrafine TiCN powder is also more likely to facilitate the rearrangement of hard phase. In this study, Cermet B4 has the highest relative density. The mixed ultrafine and micron TiCN powders under this condition not only have a better dissolution process, but also can be more conducive to the rearrangement and densification of carbonitride hard phase particles.

Fig. 4 (b) – (d) present the bending strength, hardness and fracture toughness of the TiCN-based cermets vary with the content of ultrafine TiCN powders. With the increase of the content of ultrafine TiCN powders, the hardness and bending strength of the cermet first increase and then decrease; however, the fracture toughness of the cermet increases significantly. When the mass fraction of ultrafine TiCN powder is 20 wt%, the hardness and bending strength of Cermet B4 reach the maximum value of 1 702 HV_{30} and 1 672 MPa, respectively. As compared to B6 without micron TiCN powders, they are improved by 4.0 % and 35.4 %, respectively. Compared with Cermet B1 without any addition of ultrafine TiCN powder, the hardness, bending strength and fracture toughness of Cermet B4 are improved by 2.5 %, 7.9 % and 20.4 %, respectively. When the content of the ultrafine TiCN powder is 50 wt%, the fracture toughness of Cermet B6 exhibits the highest value of 12.1 $MPa \cdot m^{1/2}$. This means that reasonable control of the micron and ultrafine TiCN powders as raw materials is beneficial to improve the hardness and bending strength of the cermets. In this study, the appropriate addition amount of ultrafine TiCN powder is 20 wt%, at which the cermet exhibits the highest hardness, bending strength and higher fracture toughness. This makes it a good candidate material in the field of high-speed cutting tools.

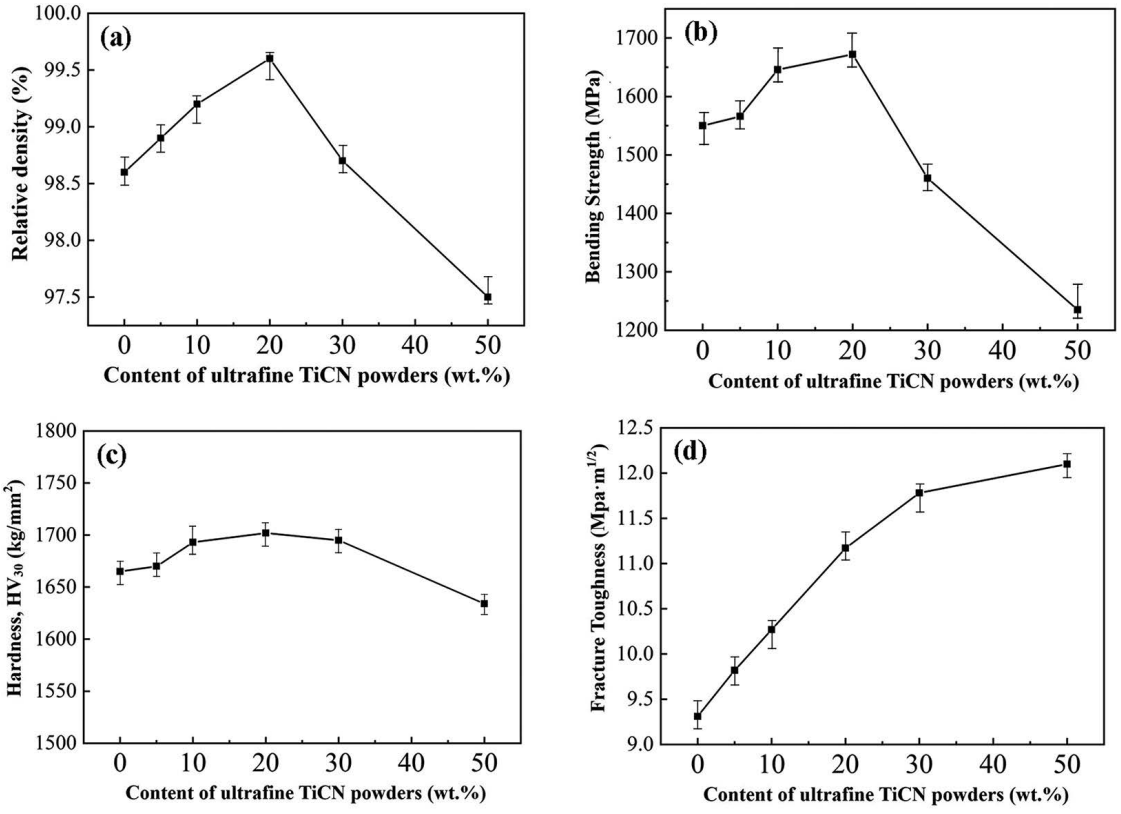

Fig. 4: The relationship of relative density (a), bending strength (b), hardness (c) and fracture toughness (d) of Cermet B1 – B6 with the content of ultrafine TiCN powders.

The mechanisms on the enhanced mechanical properties of TiCN-based cermets with the addition of ultrafine TiCN powders can be explained as follows. Firstly, the addition of ultrafine TiCN powders exerts a strong influence on the microstructures of TiCN-based cermets, as shown in Fig. 3. It is known that the black core phase in cermets consists of the undissolved TiCN grains. The oversaturated Ti, W, Mo, C and N in the liquid phase will reprecipitate on the surface of TiCN particles during the sintering process, thus forming a rim phase and inhibiting the further growth of TiCN particles [5]. With the addition of ultrafine TiCN powders, there are probably two factors that will affect the microstructures of cermets. On the one hand, the ultrafine TiCN powders have a larger specific surface compared with that of micron TiCN powders. During the liquid sintering process, the ultrafine TiCN particles are more likely to dissolve in the liquid phase to reduce the overall surface free energy, while the coarser TiCN particles will become larger by consuming the ultrafine TiCN particles on basis of the Ostwald ripening theory [28, 29]. On the other hand, the dissolved TiCN and other carbides will reprecipitate on the surface of the undissolved TiCN particles as a result of a diffusion process and interfacial reaction. This accelerates the formation of rim phase. With the addition of ultrafine TiCN powder, the rim phase on coarse TiCN particles becomes thicker and hinders the further growth of the coarse particles [5]. Therefore, as the content of ultrafine TiCN powder increases, the inhomogeneous microstructure will be introduced. The reduced average size of TiCN particles improve the hardness and bending strength of cermets [5, 30]. However, the mechanical properties deteriorate when the fraction of ultrafine TiCN powder (Fig. 4(c)) increases. This is because the rim phase that possesses lower hardness and bending strength gets thicker.

In order to explore the toughening mechanism of TiCN-based cermets, the BSE images of the crack propagation of Cermets B1, B4 and B6 are presented in Fig. 5. Cermet B1 without any addition of ultrafine TiCN powder exhibits the transgranular fracture mode (Fig. 5(a)). However, when the content of ultrafine TiCN powder is 20 wt%, both the transgranular and intergranular fracture mode can be found in Cermet B4, as shown in Fig. 5(b). It can be concluded that transgranular fracture generally occurs on coarse TiCN grains, while intergranular fracture mainly occurs on fine grains. In addition, crack deflection, crack microbridging and microcracks are also observed in Cermet B4, all of which will prevent the further propagation of cracks, thus improving the fracture toughness of the cermets. As can be seen in Fig. 3, the number of coarse TiCN particles is greatly reduced with the increased content of the ultrafine TiCN powder. Particularly, when the content of ultrafine TiCN powder is 50 wt%, a significant grain refinement phenomenon can be observed (Fig. 3(f)), which is the main reason for the maximum fracture toughness of Cermet B6 (Fig. 4(d)). Although no microcracks or crack deflection can be found in the microstructure of Cermet B6 (Fig. 5(c)), the cermet still exhibits excellent fracture toughness owing to fine grain toughening. In particular, it has been reported that the "white core-grey rim" phase can prevent the further expansion of cracks and improve the toughness of cermets because a stronger interface can be formed between the "white core-grey rim" phase and metal binder [4]. In this study, the fine "white core-grey rim" phase can be observed with the addition of ultrafine TiCN powders (Fig. 3). Moreover, with the increase of ultrafine powder, the amount of "white core-grey rim" phase also gradually increases, which is another reason why Cermet B6 exhibits the maximum fracture toughness (Fig. 4(d) and Fig. 5(c)).

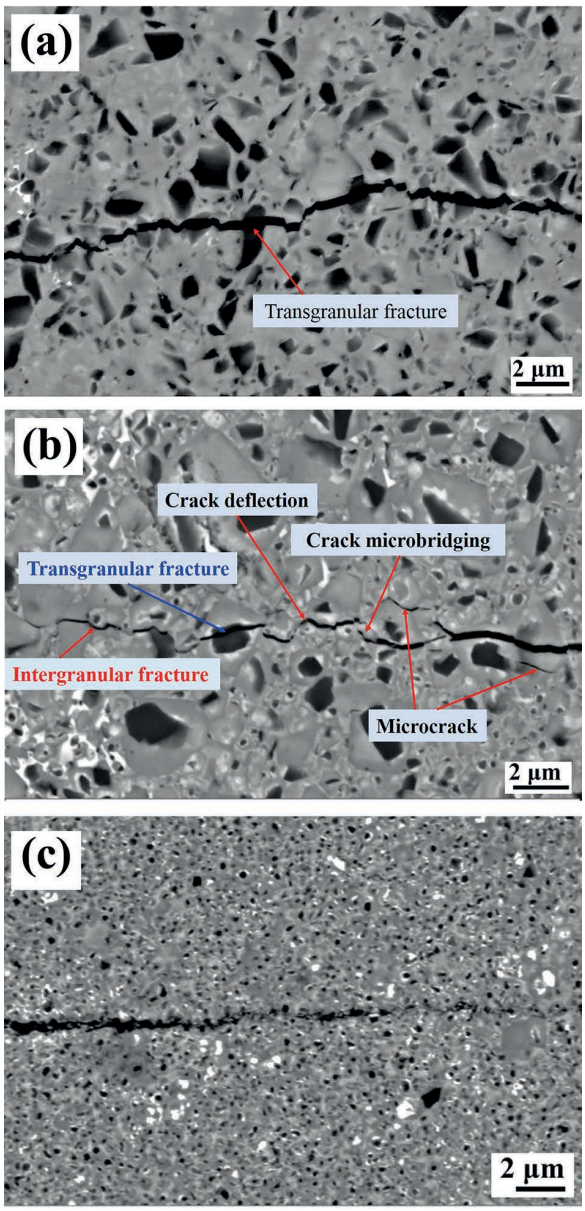

Fig. 5: The backscattered electron SEM images of the crack propagation of B1 (a), B4 (b) and B6 (c).

IV. Conclusions

TiCN-based cermets have been prepared by means of vacuum sintering technology using ultrafine TiCN powders as raw material or additives. The main conclusions of this study can be summarized as follows.

(1) The coarse (W, Mo, Ti, Nb)(Co, Ni)C phase is easily formed in TiCN-based cermets when a high WC content and coarse WC powder are used as raw material. However, finer WC powder and a lower content of WC are beneficial to promote the solid solution of W atoms.

(2) The addition of ultrafine TiCN powder as raw material can obviously refine the "black core-grey rim" phase

and promote the formation of "white core-grey rim" phase. When 20 wt% ultrafine TiCN powder was added, Cermet B4 has the highest hardness, bending strength and higher fracture toughness, which are increased by 2.5 %, 7.9 % and 20.4 % respectively, compared with cermets without the addition of ultrafine TiCN powder.

(3) The main strengthening mechanism in the as-prepared cermets is fine grain strengthening, while the toughening mechanisms include fine grain toughening, microcracks, crack deflection and crack microbridging.

Acknowledgements

This work was financially supported by the Natural Science Foundation of Fujian Provincial of China (No. 2019J01870, No. 2021J011213), and the Program for Innovative Research Team in Science and Technology in Fujian Province University.

References

1 Lengauer, W., Scagnetto, F.: Ti (C,N)-based cermets: critical review of achievements and recent developments, *Solid State Phenom.*, **274**, 53 – 100, (2018).

2 Ettmayer, P., Kolaska, H., Lengauer, W., Dreyer, K.: Ti(C,N) cermets – metallurgy and properties, *Int. J. Refract. Met. H.*, **13**, 343 – 351, (1995).

3 Xu, X., Zheng, Y., Zhang, G., Ke, Z., Wu, H., Yang, Z., Zhou, W.: Microstructure and mechanical properties of Ti(C,N)-based cermets fabricated using Ni-coated mixed powders, *Ceram. Int.*, **46**, 16944 – 16948, (2020).

4 Zhou, W., Zheng, Y., Zhao, Y., Zhang, G., Ke, Z., Yu, L.: Study on microstructure and properties of Ti(C,N)-based cermets with dual grain structure, *Ceram. Int.*, **44**, 14487 – 14494, (2018).

5 Lin, N., Zheng, Z., Zhao, L., Ma, C., Wang, Z., He, Y.: Influences of ultrafine Ti(C,N) additions on microstructure and properties of micro Ti(C,N)-based cermets, *Mater. Chem. Phys.*, **230**, 197 – 206, (2019).

6 Liu, A.J., Liu, N.: Effect of granule size and WC content on microstructure and mechanical properties of double structure Ti(C,N) based cermets, *Rare Metal Mat. Eng.*, **48**, 375 – 384, (2019).

7 Xu, X., Zheng, Y., Zhang, G., Yang, Z., Ke, Z., Wu, H., Lu, X.: Preparation of highly toughened Ti(C,N)-based cermets via mechanical activation and subsequent *in situ* carbothermal reduction, *Int. J. Refract. Met. H.*, **92**, 105310, (2020).

8 Yang, H.Y., Wang, Z., Yue, X., Ji, P.J., Shu, S.L.: Simultaneously improved strength and toughness of *in situ* bi-phased TiB_2-Ti(C,N)-ni cermets by mo addition, *J. Alloy. Compd.*, **820**, 153068, (2020).

9 Xiong, H., Xie, D., Chen, J., Chu, S., Gan, X., Li, Z., Zhou, K.: Ti(C, N)-based cermets with strengthened interfaces: roles of secondary cubic carbides, *J. Am. Ceram. Soc.*, **103**, 1582 – 1592, (2020).

10 Xiong, H., Chu, S., Lei, P., Li, Z., Zhou, K.: Ti(C,N)-based cermets containing uniformly dispersed ultrafine rimless grains: effect of VC additions on the microstructure and mechanical properties, *Ceram. Int.*, **46**, 19904 – 19911, (2020).

11 Park, S., Kang, S.: Toughened ultra-fine (Ti, W)(CN)-ni cermets, *Scripta Mater.*, **52**, 129 – 133, (2005).

12 Liu, Y., Jin, Y.Z., Yu, H.J., Ye, J.W.: Ultrafine (Ti, M) (C,N)-based cermets with optimal mechanical properties, *Int. J. Refract. Met. H.*, **29**, 104 – 107, (2011).

13 Zheng, Y., Wang, S., You, M., Tan, H., Xiong, W.: Fabrication of nanocomposite Ti(C,N)-based cermet by spark plasma sintering, *Mater. Chem. Phys.*, **92**, 64 – 70, (2005).

14 Richter, V., Ruthendorf, M.V.: On hardness and toughness of ultrafine and nanocrystalline hard materials, *Int. J. Refract. Met. H.*, **17**, 141 – 152, (1999).

15 Matsuda, T.: Effect of C/TiO_2 ratio in raw materials on thermal conductivity of titanium carbonitrides synthesized by carbothermal reduction, *J. Alloy. Compd.*, **816**, 152541, (2020).

16 Zhang, G., Zheng, Y., Zhou, W., Ke, Z., Ding, W., Yu, L., Yan, Y.: Microstructure evolution and characteristic of Ti(C,N)-based cermets prepared by *in situ* carbothermal reduction in TiO_2, *J. Am. Ceram. Soc.*, **102**, 3009 – 3018, (2019).

17 Zhang, G., Zheng, Y., Zhou, W., Zhao, Y., Zhang, J., Ke, Z., Yu, L.: Microstructure and mechanical properties of Ti(C,N)-based cermets fabricated by *in situ* carbothermal reduction of TiO_2 and subsequent liquid phase sintering, *Ceram. Int.*, **44**, 3092 – 3098, (2018).

18 Zhou, W., Zheng, Y., Zhao, Y., Zhang, G., Zhang, J.: Densification behavior, microstructure evolution and mechanical properties of Ti(C,N)-based cermets fabricated by *in situ* carbothermal reduction of WO_3 and subsequent liquid sintering, *Int. J. Refract. Met. H.*, **74**, 70 – 77, (2018).

19 Schubert, W.D., Neumeister, H., Kinger, G., Lux, B.: Hardness to toughness relationship of fine-grained WC-co hard metals, *Int. J. Refract. Met. H.*, **16**, 133 – 142, (1998).

20 Wan, W., Xiong, J., Liang, M.: Effects of secondary carbides on the microstructure, mechanical properties and erosive wear of Ti(C,N)-based cermets, *Ceram. Int.*, **43**, 944 – 952, (2017).

21 Zhang, H., Fu, M., Ma, L., Gu, S., Liu, J., Chen, Y.: Fabrication and properties of (Ti, W, mo, nb, Ta) (C,N)-Co-ni cermets, *J. Mater. Eng. Perform.*, **28**, 7198 – 7205, (2019).

22 Wang, J., Liu, Y., Ye, J., Ma, S., Pang, J.: The fabrication of multi-core structure cermets based on (Ti, W, Ta)CN and TiCN solid-solution powders, *Int. J. Refract. Met. H.*, **64**, 294 – 300, (2017).

23 Jin, Y., Liu, Y., Wang, Y., Ye, J.: Study on phase evolution during reaction synthesis of ultrafine (Ti, W, mo, V)(C, N)-ni composite powders, *Mater. Chem. Phys.*, **118**, 191 – 196, (2009).

24 Li, P., Ye, J., Liu, Y., Yang, D., Yu, H.: Study on the formation of core-rim structure in Ti(CN)-based cermets, *Int. J. Refract. Met. H.*, **35**, 27 – 31, (2012).

25 Zhang, M., Yao, H., Wang, H., Chen, Q., Bai, X., Zhao, X., Fang, Y., Xu, H., Li, Q.: *In situ* Ti(C,N)-based cermets by reactive hot pressing: reaction process, densification behavior and mechanical properties, *Ceram. Int.*, **45**, 1363 – 1369, (2019).

26 Xiong, H., Wu, Y., Li, Z., Gan, X., Zhou, K., Chai, L.: Comparison of Ti(C,N)-based cermets by vacuum and gas-pressure sintering: microstructure and mechanical properties, *Ceram. Int.*, **44**, 805 – 813, (2018).

27 Liu, N., Chao, S., Huang, X.: Effects of TiC/TiN addition on the microstructure and mechanical properties of ultra-fine grade Ti(C,N)-ni cermets, *J. Eur. Ceram. Soc.*, **26**, 3861 – 3870, (2006).

28 Marqusee, J.A., Ross, J.: Theory of ostwald ripening: competitive growth and its dependence on volume fraction, *J. Chem. Phys.*, **80**, 536 – 543, (1984).

29 Mannesson, K., Jeppsson, J., Borgenstam, A., Ågren, J.: Carbide grain growth in cemented carbides, *Acta Mater.*, **59**, 1912 – 1923, (2011).

30 Hansen, N.: Hall-petch relation and boundary strengthening, *Scripta Mater.*, **51**, 801 – 806, (2004).